# Adsorption characteristics of ciprofloxacin on the schorl: kinetics, thermodynamics, effect of metal ion and mechanisms

Danyang Yin, Zhengwen Xu, Jing Shi, Lili Shen and Zexiang He

## ABSTRACT

In this study, schorl was used as an effective adsorbent for ciprofloxacin removal from wastewater. The adsorption performance, mechanism and effect of metal ion on sorption were investigated. Adsorption capacity reached a maximum (8.49 mg/g) when the pH value was 5.5. The pseudo-second-order kinetic model and Freundlich model could better describe the experimental data. The negative ΔH (–22.96 KJ/mol) value showed that the adsorption process was exothermic. The results also indicated physical adsorption existed on the adsorption process, which was in agreement with the analysis of X-ray diffraction, scanning electron microscopy, Fourier transform infrared spectroscopy (FTIR) and X-ray photoelectron spectroscopy. The desorption rate could reach 94%, which suggested that schorl had a good desorption and regeneration performance. Coexisting ions, such as $Cu^{2+}$ and $Al^{3+}$, could obviously inhibit adsorption, and the inhibition from $Al^{3+}$ was significantly higher than that from $Cu^{2+}$. However, the additional $Zn^{2+}$ could slightly promote the adsorption.

**Key words** | adsorption, ciprofloxacin, coexisting ions, pH, schorl

**Danyang Yin**
**Jing Shi** (corresponding author)
**Lili Shen**
**Zexiang He**
Department of Environmental Science,
China Pharmaceutical University,
211198 Nanjing,
China
E-mail: *shijing_cpu@163.com*

**Zhengwen Xu**
Jiangsu Collaborative Innovation Center of Atmospheric Environment and Equipment Technology,
Nanjing University of Information Science & Technology,
210044 Nanjing,
China

**Danyang Yin**
**Zhengwen Xu**
School of Environmental Science and Engineering,
Nanjing University of Information Science & Technology,
210044 Nanjing,
China

## INTRODUCTION

Ciprofloxacin (CIP), a synthetic antibiotic, is a typical kind of fluoroquinolone (FQ) (Picó & Andreu 2007; Li *et al.* 2013). It is utilized for the inhibition of some diseases for humans and animals. However, because of the continuous increment of production amount and inappropriate discharge (Zhang & Huang 2007; Yang *et al.* 2010; Zhang *et al.* 2015), a series of problems occurred. As in previously published results, it is frequently detected in the environment (Kolpin *et al.* 2002; Martins *et al.* 2008). In pharmaceutical wastewater, the concentrations of CIP are as high as 28–31 mg $L^{-1}$ (Larsson *et al.* 2007). Prolonged exposure to CIP could promote antibiotic-resistance of bacteria and their high potential risks to ecological and human health (Jiao *et al.* 2008; Kemper 2008). However, due to the low biodegradation rate and bacteria-inhibition effect, it was difficult to be removed by traditional biological wastewater treatment processes (Sarmah *et al.* 2006; Teske & Arnold 2008). Consequently, it is vital to determine an effective method for the disposal of CIP in wastewater.

In the past decades, several conventional processes such as biodegradation, chemical oxidation and adsorption were applied for the treatment of CIP in the solution (Li & Zhang 2010, Benitez *et al.* 2011, Hu & Wang 2016; Yu *et al.* 2016). Among these treatments, the adsorption process acquires a special importance because of the inexpensive nature and ease of operation. Natural minerals, such as aluminous



doi: 10.2166/wrd.2017.143

oxide, magnetite, were often chosen as model sorbents for the removal of CIP from wastewater. The adsorption capacities of aluminous oxide and magnetite reached 13.6 and 12.7 mg/g, respectively (Gu & Karthikeyan 2005; Rakshit *et al.* 2013). These results demonstrated that minerals play an important role in the adsorption of CIP from aqueous solution. Hence, the natural adsorbents with low cost, simple process, good feasibility and high adsorption capacity are needed.

Tourmaline is a borosilicate mineral that consists of variable elements. The general chemical formula of tourmaline can be represented as $XY_3Z_6[Si_6O_{18}][BO_3]W_4$ (in which X is $Na^+$, $Ca^{2+}$ or vacancies; Y is $Fe^{2+}$; Z is $Al^{3+}$, $Mg^{2+}$, $Fe^{3+}$; W is OH, F, O). If size Y was occupied by a different element, the tourmaline could be divided into olenite (Al tourmaline), dravite (Mg tourmaline), alkali tourmaline and schorl (Fe tourmaline). The crystal structure of schorl belongs to the trigonal space group. Schorl also has a special property of spontaneous and permanent poles, which could produce an electric dipole. Hence, an electric field exists on the surface of the schorl granule (Nakamura & Kubo 1992; Xia *et al.* 2006; Wang *et al.* 2012). In addition, schorl can release negative ions. These unique features of schorl mean it can be widely used in various fields (Sergei & Alice 2002; Xu *et al.* 2009; Liu *et al.* 2013; Wang *et al.* 2013; Yu *et al.* 2014). Schorl was capable of adsorbing dyestuff and heavy metal ions (Guerra *et al.* 2012; Liu *et al.* 2016). However, there has been no research focusing on the disposal of antibiotics, especially CIP, by the adsorption onto schorl. If the schorl could remove CIP effectively by adsorption, it would expand its application. Moreover, because it is a low cost natural mineral and does not need to be modified further, it will not have problems such as secondary pollutions in some other chemical removal approaches.

The objective of this paper was to investigate the adsorption characteristics of CIP onto schorl. The affecting factors, such as pH, temperature and coexisting ions were investigated in the experiments. The adsorption isotherms and kinetics equations were used to explain adsorption performances. Efficient regeneration of the schorl adsorbent was also observed. This paper can provide a scientific basis and practical technology for the treatment of CIP in wastewater.

## MATERIALS AND METHODS

### Materials

Aluminum chloride hexahydrate, zinc chloride, copper chloride dihydrate, hydrochloric acid, and sodium hydroxide were of analytical reagents grade and were obtained from Nanjing Wanqing Chemical Co., Ltd (Nanjing, China). Ciprofloxacin hydrochloride ($C_{17}H_{18}FN_3O_3$.HCl, purity >98%) was purchased from Sigma-Aldrich, the molecular structure of ciprofloxacin is given in Figure 1. The schorl was obtained from Xinjiang Province of China.

### Batch sorption experiments

All the adsorption experiments were carried out in 250 mL Erlenmeyer flasks with 0.1 g schorl, and 50 mL CIP solution was added. pH value was adjusted with 0.1 mol/L NaOH or 0.1 mol/L HCl. The mixtures were shaken at 240 rpm at different temperatures for 12 h. When it reached equilibrium, the solution was passed through a 0.22 μm filter before analysis. In the kinetic experiments, water samples were taken at predetermined time intervals. For the isotherm studies, the experiments were operated at different temperatures (288, 303 and 318 K). In order to determine the effect of heavy metal ions on the adsorption, the heavy metal ions were added into the CIP solutions (30 mg/L) according to certain mole ratios (CIP:M = 1:0, 1:1, 1:2, 1:5, 1:10). The desorption experiment was performed after the adsorption experiments, by adjusting the pH to 11 with 1 mol/L NaOH solution. The flasks were sealed and shaken at a speed of 240 rpm for 12 h. The CIP concentration was determined by a UV–Vis spectrophotometer (UV-1800) at a wavelength of 275 nm (Sun *et al.* 2016).

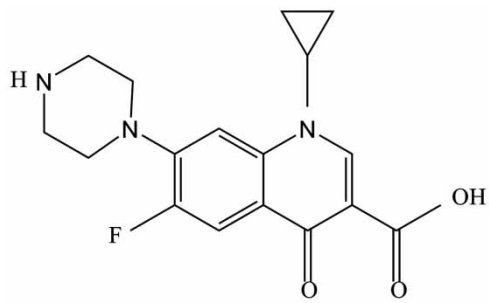


**Figure 1** | The structure of CIP.

### Characterization methods

The original and absorbed samples were analyzed by X-ray diffraction (XRD), scanning electron microscopy (SEM), X-ray photoelectron spectroscopy (XPS) and Fourier transform infrared spectroscopy (FTIR) analyses. The structure of the samples was performed on an XRD-6100 diffractometer with Ni-filtered Cu Ka radiation, operating at 40 kV and 50 mA. The samples were scanned in the range of 10–80° (2θ) at a scanning rate of 7 $min^{-1}$. SEM (Hitachi SU-1510) was operated with an acceleration voltage of 15 keV. The samples were measured on a VG ESCALAB MKII XPS system with Mg $K_\alpha$ source and a charge neutralizer. The FTIR spectra were obtained on NiCOLET iS5 spectrometer. The spectra were collected by accumulating 250 scans at a resolution of 4 $cm^{-1}$ in the range of 400–4,000 $cm^{-1}$.

### Data analysis

The adsorption rate is one of the important parameters that affect the adsorption process (Srivastava *et al.* 2006; Hao *et al.* 2012). To characterize the adsorption process of CIP on the schorl, pseudo-first-order and pseudo-second-order kinetic models were applied to fit the experimental data. The equations can be represented as follows (Wan *et al.* 2013).

Pseudo-first-order kinetic model:

$$q_t = q_e\left(1 - e^{-k_1 t}\right) \tag{1}$$

Pseudo-second-order kinetic model:

$$q_t = \frac{k_2 q_e^2 t}{1 + k_2 q_e t} \tag{2}$$

where $q_t$ (mg·$g^{-1}$) and $q_e$ (mg·$g^{-1}$) are the adsorption capacity of schorl at any time $t$ (min) and the equilibrium adsorption capacity of schorl, respectively; $k_1$ ($min^{-1}$) and $k_2$ (g·$mg^{-1}$·$min^{-1}$) are the adsorption rate constants of pseudo-first-order and pseudo-second-order equations, respectively.

Adsorption isotherms were used to evaluate the interaction between the adsorbent and the adsorbate. To further understand the adsorption mechanism, two typical models, Langmuir and Freundlich, were selected to analyze isotherm data and the expressions can be written as follows (Foo & Hameed 2010).

Langmuir isotherm model:

$$q_e = \frac{k_L q_m c_e}{1 + k_L c_e} \tag{3}$$

Freundlich isotherm model:

$$q_e = k_F c_e^{1/n} \tag{4}$$

where $q_m$ is the maximum adsorption capacity (mg.$g^{-1}$); $c_e$ is the equilibrium concentration of CIP (mg.$L^{-1}$); $k_L$ is the Langmuir equilibrium constant; $k_F$ is Freundlich isotherm constants, which are indicative of the affinity of the binding sites; $n$ is the nonlinearity constant reflecting the favorability of adsorption and the degree of surface heterogeneity and both were related to the adsorption capacity and intensity.

The thermodynamic parameters represent the change in free energy (ΔG), enthalpy (ΔH), and entropy (ΔS) of the adsorption process was obtained from the temperature-dependent isotherms by using the Van't-Hoff equation:

$$\Delta G = -RT \ln K \tag{5}$$

$$\ln K = \frac{\Delta S}{R} - \frac{\Delta H}{RT} \tag{6}$$

in which $R$ is the gas constant (8.314 J/mol K), T is the absolute temperature (K); and $K$ is the adsorption constant in the Langmuir equation, L/mol (Liu 2009); ΔG is the Gibbs free energy change, kJ/mol; ΔH is the standard enthalpy change, kJ/mol; ΔS is the entropy change, kJ/mol. The values of ΔH and ΔS were calculated from the slope and intercept of the plot of ln$K$ versus 1/T.

## RESULTS AND DISCUSSION

### Kinetic studies

The effect of contact time on CIP adsorption is shown in Figure 2. The adsorption capacity was increased quickly,

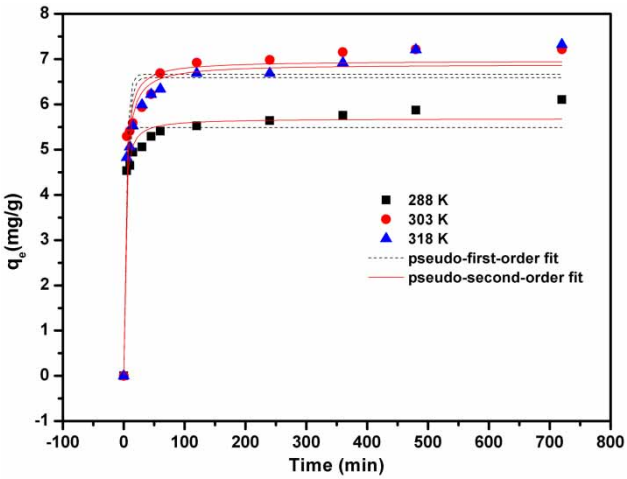


**Figure 2** | Adsorption kinetics of CIP on the schorl.

reaching about 75% of the finally adsorbed amounts during the initial 10 min. After this period, the adsorption rate was gradually slow and reached equilibrium in about 120 min. The adsorption capacity of CIP reached 7.2 mg/g. To further evaluate the adsorption kinetics of CIP on the schorl, pseudo-first-order and pseudo-second-order kinetic models were employed to fit the experimental data. The parameters are listed in Table 1. In comparison with the pseudo-first-order kinetic model, the pseudo-second-order kinetic model had a higher correlation coefficient value to describe experimental data. The results were similar to the adsorption of CIP onto activated carbons, ordered mesoporous carbon, bamboo-based carbon and layered chalcogenides (Li *et al.* 2015b; Peng *et al.* 2015; Sun *et al.* 2016). Furthermore, the theoretical values of $q_e$ in the pseudo-second-order kinetics were closer to the experimental $q_e$ than pseudo-first-order kinetics. In conclusion, the above results suggested that the adsorption process were well represented by the pseudo-second-order kinetic model.

**Table 1** | Kinetics constants and correlation coefficients for the adsorption of CIP by the schorl

| | Pseudo-first-order model | | | Pseudo-second-order model | | |
|---|---|---|---|---|---|---|
| T (K) | $k_1$ ($min^{-1}$) | $q_e$ (mg/g) | $R^2$ | $k_2$ ($g \cdot mg^{-1} \cdot min^{-1}$) | $q_e$ (mg/g) | $R^2$ |
| 288 | 0.289 | 5.49 | 0.943 | 0.0999 | 5.69 | 0.979 |
| 303 | 0.238 | 6.68 | 0.914 | 0.0599 | 6.97 | 0.970 |
| 318 | 0.191 | 6.60 | 0.924 | 0.0486 | 6.89 | 0.976 |

## Adsorption isotherms and thermodynamics

The adsorption isotherms of CIP absorbed on the schorl at different temperatures is shown in Figure 3. The equilibrium concentration of CIP increased with the increasing initial concentration. Isotherm parameters and the correlation coefficients are shown in Table 2. The adsorption process fits better with the Freundlich model in comparison to the Langmuir model, indicating multilayer physical adsorption. In the Langmuir model, the largest adsorption capacity $q_m$ was increased slightly from 8.54 to 9.68 mg/g with the increasing temperature, which suggested that temperature has little effect on the adsorption process. Schorl exhibited a lower adsorption capacity of CIP compared to CIP adsorbed on magnetite, aluminous oxide, ordered mesoporous carbon, bamboo-based carbon and layered chalcogenides, while it showed a higher adsorption amount in comparison with modified coal fly ash, zetolite

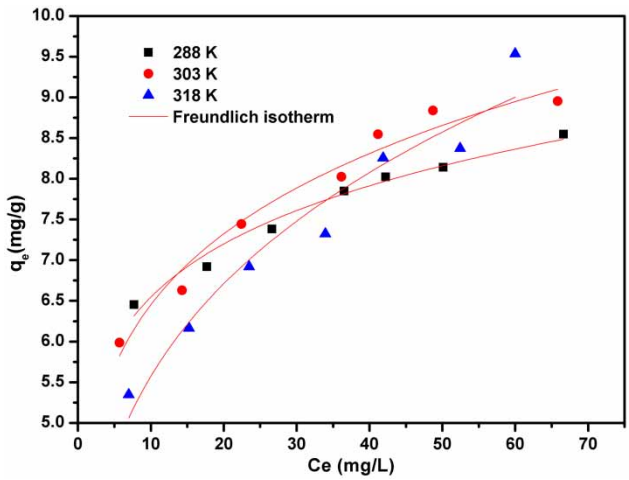


**Figure 3** | Adsorption isotherms of CIP on the schorl.

**Table 2** | The parameters of adsorption isotherms of CIP on the schorl at different temperature

| | Langmuir model | | | Freundlich model | | |
|---|---|---|---|---|---|---|
| T (K) | $q_m$ (mg/g) | $K_L$ | $R^2$ | $K_F$ | n | $R^2$ |
| 288 | 8.54 | 0.336 | 0.823 | 4.778 | 7.30 | 0.977 |
| 303 | 9.16 | 0.262 | 0.805 | 4.24 | 5.46 | 0.966 |
| 318 | 9.68 | 0.134 | 0.805 | 3.01 | 3.75 | 0.937 |

and kaolinite (Table 3). As for the Freundlich model, all the constants $n$ were greater than 1, giving an indication for the favorability of adsorption.

The thermodynamic parameters were calculated from the Van't-Hoff equation. As shown in Table 4, the negative G values demonstrated that CIP absorbed on the schorl was a spontaneous process. As in previous studies, if the absolute value of ΔG was in the range of 2.1–20.9 KJ/mol, it was indicative of physical adsorption existing in the adsorption process, while it was between 80 and 200 KJ/mol, the adsorption should be associated with chemical adsorption (Liu & Liu 2008; Wu *et al.* 2016). The values of ΔG at different temperatures in this study were in the range between those of physical adsorption and chemical adsorption. Hence, CIP absorbed on schorl could be regarded as a physical adsorption enhanced by the electrostatic effect. The negative value of ΔH indicated that the adsorption process was exothermic. The ΔH evolved during adsorption were less than 40 KJ/mol, which was in agreement with the observed physical adsorption (Zhang *et al.* 2009; Sadasivam *et al.* 2010). The positive ΔS (0.0188 KJ/mol) value for CIP adsorption suggested an increase in the randomness at solid–solute interface during the adsorption process.

**Table 3** | Comparison of maximum adsorption capacity (q max) of various adsorbents for CIP

| Adsorbent | $q_m$ (mg/g) | Reference |
|---|---|---|
| Modified coal fly ash | 1.547 | Zhang *et al.* (2011) |
| Zeolite | 5.79 | Genç & Dogan (2015) |
| Kaolinite | 6.3 | Li *et al.* (2011) |
| Schorl | 8.48 | This study |
| Magnetite | 12.73 | Rakshit *et al.* (2013) |
| Aluminous oxide | 13.6 | Gu & Karthikeyan (2005) |
| Layered chalcogenides | 230.9 | Li *et al.* (2015b) |
| Ordered mesoporous carbon | 233.37 | Peng *et al.* (2015) |
| Bamboo-based carbon | 362.94 | Peng *et al.* (2015) |

**Table 4** | The calculated values of thermodynamic parameters of CIP on the schorl

| T (K) | ΔG (kJ·mol$^{-1}$) | ΔH (kJ·mol$^{-1}$) | ΔS (kJ·mol$^{-1}$) |
|---|---|---|---|
| 288 | –28.19 | –22.96 | 0.0188 |
| 303 | –29.03 | | |
| 318 | –28.71 | | |

## Effect of the pH

Previous studies reported that the pH has a major impact on adsorption (Gu & Karthikeyan 2005; Vasudevan *et al.* 2009). In the schorl system, the effect of pH on the CIP adsorption is shown in Figure 4. Adsorption capacity increased with the increasing pH and reached a maximum capacity (8.49 mg/g) at pH 5.5, then it decreased with the increment of pH value. It was dependent on the charge of schorl and the speciation of CIP molecule under different pH values.

The pH value of solution could affect both surface charge and density of the schorl, as well as the degree of protonation of the CIP. The schorl surface is, overall, negatively charged at pH > 2.5 ($pH_{pzc}$) over the whole pH range, whereas CIP ($pK_{a1} = 6.1$, $pK_{a2} = 8.7$) exhibited pH-dependent speciation in its different forms as a cation (<6.1), zwitterion (6.1–8.7), and anion (>8.7) (Hongsawat *et al.* 2014). When the pH < $pK_{a1}$, the cation was the dominant ciprofloxacin species in aqueous solution. CIP adsorbed onto schorl was primarily via electrostatic attraction between negative sites of schorl and piperazinyl groups of CIP. At the lower pH (pH = 3), the adsorption capacity was lower due to the weaker electrostatic attraction between

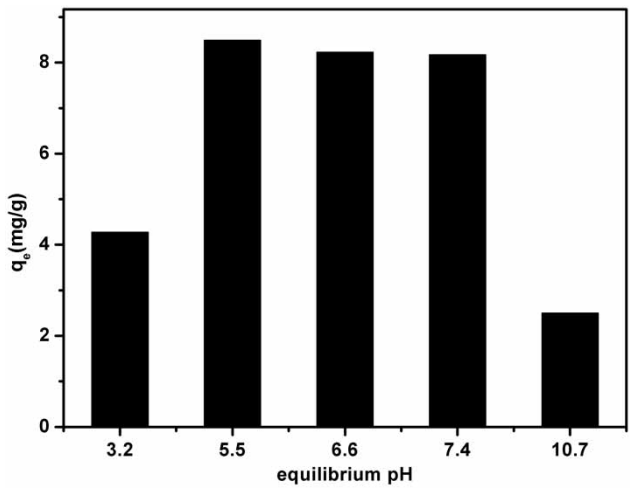


**Figure 4** | Effect of initial pH on CIP adsorption by schorl ($[CIP]_{initial}$ = 50 mg/L, T = 303 K).

the lower negatively charged of the schorl and $CIP^+$. In addition, the existence of $H^+$ would also affect CIP absorbed on schorl. When the pH was between $pK_{a1}$ and $pK_{a2}$, CIP existed as the zwitterion forms and adsorption capacities of the CIP decreased. At pH $>pK_{a2}$, a sharp decrease was observed, which could be attributed to electrostatic repulsion. This result was in agreement with the ciprofloxacin adsorption on kaolinite (Li *et al.* 2011).

## XRD, SEM, FTIR, XPS analysis

The XRD patterns of the schorls before and after adsorption are shown in Figure 5. The schorl matched with the standard card (No.43-1464), indicating that it was the typical pattern of schorl. It was observed that after adsorption the schorl shared the same characteristic diffraction peaks with the original schorl. No differences were found between the samples before and after adsorption. The SEM images are shown in Figure 6, the original schorl particles (Figure 6(a)) presented various shapes and the size was approximately 1–17 μm. As illustrated in Figure 6(b), the morphology of the absorbed schorl was almost the same as the original schorl. As can be seen from Figure 7, the peak at ~424 $cm^{-1}$, considered as the stretching O-Fe-O vibration at octahedral sites (Nadeem *et al.* 2010), the peak at ~506, 705 and 1,028 $cm^{-1}$ were the function groups of Si-O, O-Si-O, Si-O-Si (Mitra *et al.* 2007). The band at 1,267 $cm^{-1}$ was a result of stretching vibration of B-O bonds. The peak at 3,559 $cm^{-1}$ is attributed to O–H bond

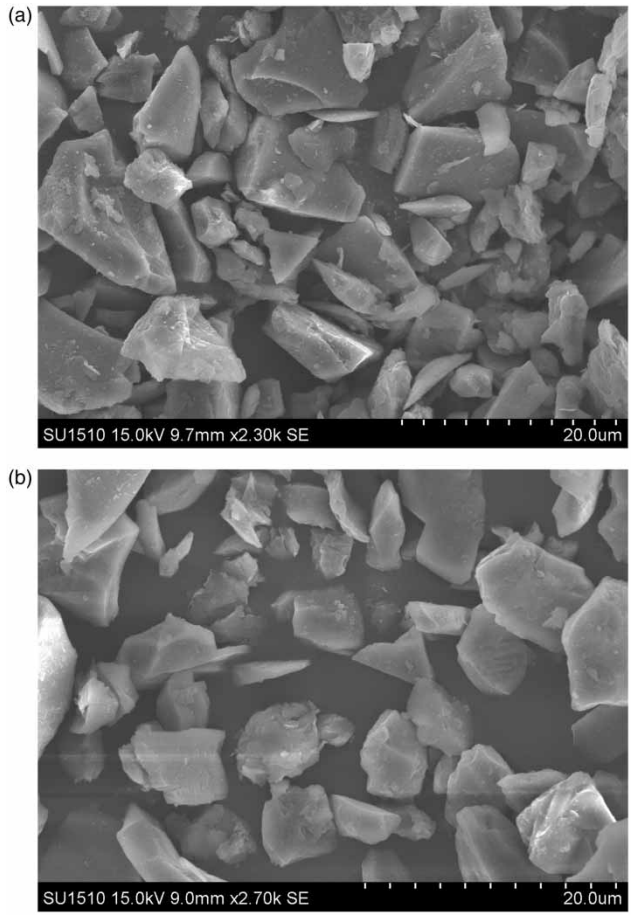


**Figure 6** | The SEM images of the original schorl (a) and the absorbed schorl (b).

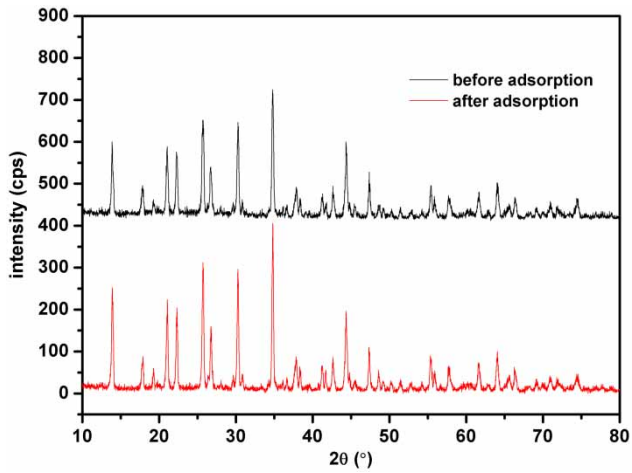


**Figure 5** | XRD patterns of the schorl and the absorbed schorl.

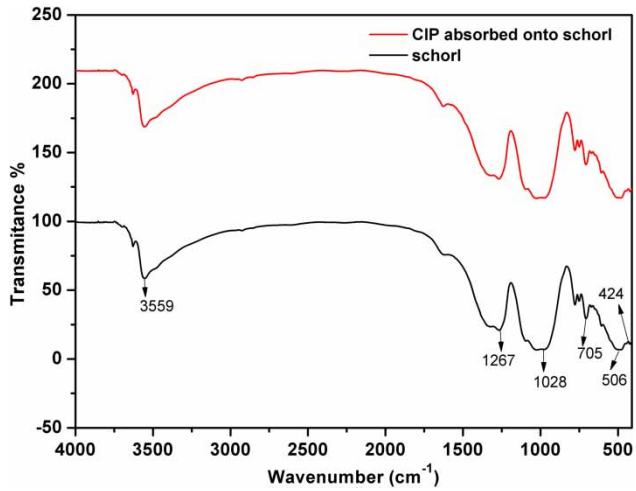


**Figure 7** | FTIR spectra of schorl before and after CIP adsorption.

stretching (Li *et al.* 2015a). No new absorption peaks and peak shift phenomenon appeared on the FTIR of schorl after adsorption in the relevant wavelength region, indicating that the adsorption may be a physical adsorption.

XPS analysis was employed to ascertain the surface chemical composition of the samples. The bonding energies (BE) of 284.8, 532.1, 685.5, 74.8, and 102.8 eV corresponded to $C_{1S}$, $O_{1S}$, $F_{1S}$, $Al_{2p}$, and $Si_{2p}$ groups of schorl, respectively, and the $Fe_{2p}$ values were 711.3 and 724.8 eV. After adsorption, the new peaks formed, which were consistent with BE values of CIP (Polishchuk *et al.* 2009), demonstrating that CIP was successfully adsorbed onto the schorl. In comparison with the BE values of schorls before and after adsorption, except for the new peaks from the adsorbed CIP, they were almost not changed (±0.2 eV) (Table 5). Hence, it was demonstrated CIP absorbed on schorl, probably due to physical adsorption.

## Desorption experiment

The desorption rate is an important index to measure the recycling of adsorption materials. After the process of adsorption, the desorption experiment is performed by adjusting the pH to 11, and the result is shown in Figure 8. Obviously, a large portion of CIP was quickly desorbed from schorl in 20 minutes. The desorption rate reached 94%, which indicated that schorl had a good desorption ability simply by adjusting the pH values to 11. Electrostatic repulsion could be attributed to the CIP desorption at a high pH value.

**Table 5** | Binding energies of elements in the schorl, CIP absorbed on schorl, CIP

| | Schorl before adsorption | Schorl after adsorption | CIP |
|---|---|---|---|
| C | 284.8 | 284.8 | 284.8 |
| | | 286.4 | 286.3 |
| F | 685.5 | 685.4 | |
| | | 687.4 | 687.3 |
| N | 400.7 | 399.9 | 399.8 |
| | | 401.4 | 401.2 |
| | | 531.3 | 531.3 |
| O | 532.1 | 532.1 | |
| | | 532.7 | 532.7 |
| Si | 102.8 | 102.8 | |
| Al | 74.8 | 74.7 | |
| Fe | 711.3 | 711.1 | |
| | 724.8 | 724.7 | |

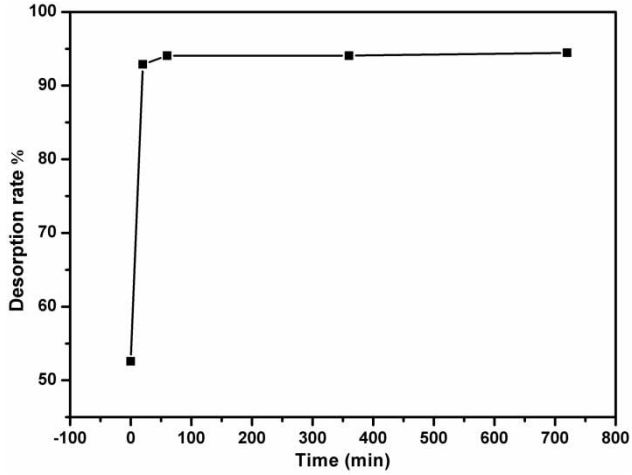


**Figure 8** | Desorption of CIP by schorl on alkaline condition.

## Effect of coexisting ions

Several studies found that the concentrations of heavy metals in the solution could affect the adsorption capacity of CIP. In the presence of heavy metal ion, the CIP adsorption capacity changed, as illustrated in Figure 9.

$Zn^{2+}$ had a weak impact on CIP adsorption. The existence of $Zn^{2+}$ enhanced the CIP adsorption slightly. It is possible that CIP was adsorbed on schorl via $Zn^{2+}$ bridging,

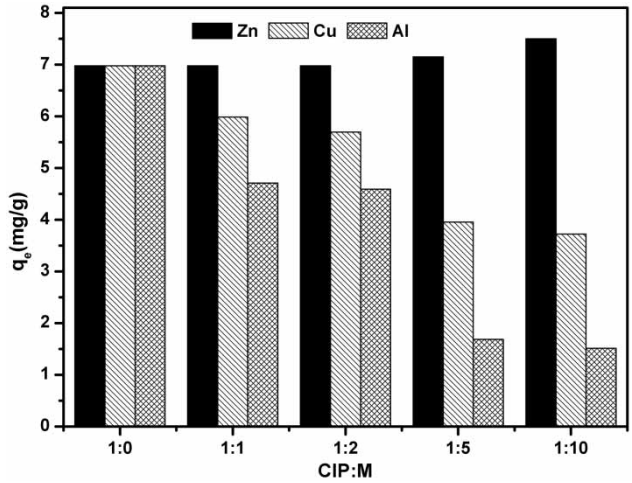


**Figure 9** | Effect of coexisting ions on the adsorption of CIP on the schorl ($[CIP]_{initial}$ = 30 mg/L, pH = 5.5, T = 303 K).

a part of $Zn^{2+}$ interacted with CIP to form complexes with a positive surface charge, which were more easily adsorbed on the surface of schorl, similar to the results of enrofloxacin sorbed onto a calcareous soil in the presence of $Zn^{2+}$ (Graouer-Bacart *et al.* 2015).

On the contrary, the addition of $Cu^{2+}$ or $Al^{3+}$ obviously inhibited the adsorption. When the mole ratios were 1:1 (CIP: Cu or CIP: Al), the adsorption amounts of CIP were 5.99 and 4.71 mg/g, respectively. Furthermore, with higher concentrations of $Cu^{2+}$ or $Al^{3+}$, the adsorption capacity decreased further. The possible reason could be explained by two aspects: one is that heavy metal ions may compete with CIP for the active site on schorl surface (Jiang *et al.* 2006) and the other possible reason is that the formation of metal complexes has a lower affinity for the schorl surface than the CIP alone. This observation was similar to the result of $Cu^{2+}$ which could decrease the CIP adsorption on sand media via competing adsorption under pH = 5.6 conditions (Chen *et al.* 2013). However, several studies pointed out that the presence of $Cu^{2+}$ promoted sorption onto both kaolinite and montmorillonite (Pei *et al.* 2009). This may be related to the different characteristics of the minerals. In the same mole ratios, the inhibition from $Al^{3+}$ was significantly higher than that from $Cu^{2+}$. The reason may be concluded that the charge of the $Al^{3+}$ leads to a higher affinity to the surface of schorl than $Cu^{2+}$.

### UV–visible spectroscopy

The spectrum of CIP after reaction and the solution of CIP adsorbed onto schorl in the presence of $Zn^{2+}$, $Cu^{2+}$ and $Al^{3+}$ respectively, are shown in Figure 10. Pure ciprofloxacin exhibited three absorption bands at around 275, 315 and 323 nm. It was observed that the bathochromic shift observed from 275 to 278 nm in the presence of $Cu^{2+}$ and $Al^{3+}$ on CIP adsorption after the reaction. According to the adsorption study (Zhang *et al.* 2012; Muthumariappan 2013), a large portion of CIP could exist in the form of complexes with metallic cations ($Cu^{2+}$, $Al^{3+}$) in the solution. The result was similar to that of the adsorbed tetracycline onto zeolite beta (Kang *et al.* 2011). However, no absorbance peaks were shifted with the existence of $Zn^{2+}$ in CIP solution, indicating no generation of ciprofloxacin zinc complex. This result verified the fact that CIP adsorbed on schorl via $Zn^{2+}$ bridging on the above.

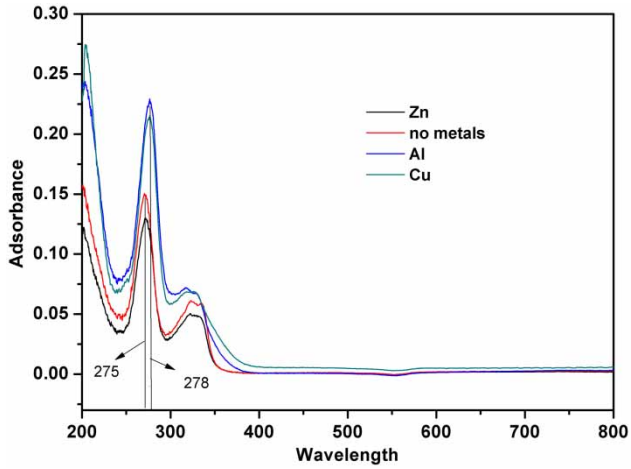


**Figure 10** | UV–Visible spectra of reaction solution under different conditions.

## CONCLUSIONS

In the experiment, schorl was an effective adsorbent for ciprofloxacin removal from the solution. When the equilibrium pH value was 5.5, the maximum adsorption capacity was found to be 8.49 mg/g. The pseudo-second-order kinetic model and Freundlich model could well describe the experimental data. The negative ΔG and ΔH value indicated that the adsorption process was spontaneous and exothermic and it was physical adsorption. The analysis of XRD, SEM, FTIR and XPS were in good agreement with physical adsorption. The existence of $Cu^{2+}$ and $Al^{3+}$ has a negative effect on the ciprofloxacin adsorption, and the inhibition by the $Al^{3+}$ was significantly higher than that by $Cu^{2+}$. However, the addition of $Zn^{2+}$ could slightly promote ciprofloxacin adsorption capacity. The desorption experiment indicated that schorl had a good desorption and regeneration performance.

## ACKNOWLEDGEMENTS

This research was supported by the National Natural Science Foundation of China (51408612), the Natural Science Foundation of Jiangsu Province (BK20140660),

the Qing Lan Project, the Fundamental Research Funds for the Central Universities (2015PT002) and the College Students Innovation Project for the R&D of Novel Drugs (J1310032).

## REFERENCES


Benitez, F. J., Acero, J. L., Real, F. J., Roldan, G. & Casas, F. 2011 Comparison of different chemical oxidation treatments for the removal of selected pharmaceuticals in water matrices. *Chem. Eng. J.* **168** (3), 1149–1156.

Chen, H., Ma, L. Q., Gao, B. & Gu, C. 2013 Effects of Cu and Ca cations and Fe/Al coating on ciprofloxacin sorption onto sand media. *J. Hazard. Mater.* **225–232**, 375–381.

Foo, K. Y. & Hameed, B. H. 2010 Insights into the modeling of adsorption isotherm systems. *Chem. Eng. J.* **156** (1), 2–10.

Genç, N. & Dogan, E. C. 2015 Adsorption kinetics of the antibiotic ciprofloxacin on bentonite, activated carbon, zeolite, and pumice. *Desalin. Water Treat.* **53** (3), 785–793.

Graouer-Bacart, M., Sayen, S. & Guillon, E. 2015 Adsorption of enrofloxacin in presence of Zn (II) on a calcareous soil. *Ecotoxicol. Environ. Saf.* **122**, 470–476.

Gu, C. & Karthikeyan, K. G. 2005 Sorption of the antimicrobial ciprofloxacin to aluminum and iron hydrous oxides. *Environ. Sci. Technol.* **39** (23), 9166–9173.

Guerra, D. L., Oliveira, S. P., Silva, R. A. R., Leidens, V. & Batista, A. C. 2012 Characterization and application of tourmaline and beryl from Brazilian pegmatite in adsorption process with divalent metals. *Int. J. Mining Sci. Technol.* **22** (5), 711–718.

Hao, S., Zhong, Y., Pepe, F. & Zhu, W. 2012 Adsorption of $Pb^{2+}$ and $Cu^{2+}$ on anionic surfactant-templated amino-functionalized mesoporous silicas. *Chem. Eng. J.* **189**, 160–167.

Hongsawat, P., Prarat, P., Ngamcharussrivichai, C. & Punyapalakul, P. 2014 Adsorption of ciprofloxacin on surface functionalized superparamagnetic porous silicas. *Desalin. Water Treat.* **52** (22–24), 4430–4443.

Hu, D. & Wang, L. 2016 Adsorption of ciprofloxacin from aqueous solutions onto cationic and anionic flax noil cellulose. *Desalin. Water Treat.* **57** (58), 1–14.

Jiang, K., Sun, T., Sun, L. & Li, H. 2006 Adsorption characteristics of copper, lead, zinc and cadmium ions by tourmaline. *J. Environ. Sci.* **18** (6), 1221–1225.

Jiao, S. J., Zheng, S. R., Yin, D. Q., Wang, L. H. & Chen, L. Y. 2008 Aqueous oxytetracycline degradation and the toxicity change of degradation compounds in photoirradiation process. *J. Environ. Sci.* **20** (7), 806–813.

Kang, J., Liu, H. J., Zheng, Y. M., Qu, J. H. & Chen, J. P. 2011 Application of nuclear magnetic resonance spectroscopy, Fourier transform infrared spectroscopy, UV–Visible spectroscopy and kinetic modeling for elucidation of adsorption chemistry in uptake of tetracycline by zeolite beta. *J. Colloid Interface Sci.* **354** (1), 261–267.

Kemper, N. 2008 Veterinary antibiotics in the aquatic and terrestrial environment. *Ecol. Indic.* **8** (1), 1–13.

Kolpin, D. W., Furlong, E. T., Meyer, M. T., Thurman, E. M., Zaugg, S. D., Barber, L. B. & Buxton, H. T. 2002 Pharmaceuticals, hormones, and other organic wastewater contaminants in US streams, 1999–2000: a national reconnaissance. *Environ. Sci. Technol.* **36** (6), 1202–1211.

Larsson, D. J., de Pedro, C. & Paxeus, N. 2007 Effluent from drug manufactures contains extremely high levels of pharmaceuticals. *J. Hazard. Mater.* **148** (3), 751–755.

Li, B. & Zhang, T. 2010 Biodegradation and adsorption of antibiotics in the activated sludge process. *Environ. Sci. Technol.* **44** (9), 3468–3473.

Li, Z., Hong, H., Liao, L., Ackley, C. J., Schulz, L. A., MacDonald, R. A., Ackley, C. J., Schulz, L. A., MacDonald, R. A., Mihelich, A. L. & Emard, S. M. 2011 A mechanistic study of ciprofloxacin removal by kaolinite. *Colloids Surf. B* **88** (1), 339–344.

Li, W., Shi, Y., Gao, L., Liu, J. & Cai, Y. 2013 Occurrence, distribution and potential affecting factors of antibiotics in sewage sludge of wastewater treatment plants in China. *Sci. Total Environ.* **445**, 306–313.

Li, G., Chen, D., Zhao, W. & Zhang, X. 2015a Efficient adsorption behavior of phosphate on La-modified tourmaline. *J. Environ. Chem. Eng.* **3** (1), 515–522.

Li, J. R., Wang, Y. X., Wang, X., Yuan, B. & Fu, M. L. 2015b Intercalation and adsorption of ciprofloxacin by layered chalcogenides and kinetics study. *J. Colloid Interface Sci.* **453**, 69–78.

Liu, Y. 2009 Is the free energy change of adsorption correctly calculated? *J. Chem. Eng. Data* **54** (7), 1981–1985.

Liu, Y. & Liu, Y. J. 2008 Biosorption isotherms, kinetics and thermodynamics. *Separ. Purif. Technol.* **61** (3), 229–242.

Liu, H., Wang, C., Liu, J., Wang, B. & Sun, H. 2013 Competitive adsorption of Cd (II), Zn (II) and Ni (II) from their binary and ternary acidic systems using tourmaline. *J. Environ. Manage.* **128**, 727–734.

Liu, N., Wang, H., Weng, C. H. & Hwang, C. C. 2016 Adsorption characteristics of Direct Red 23 azo dye onto powdered tourmaline. *Arab. J. Chem.* dx.doi.org/10.1016/j.arabjc.2016.04.010.

Martins, A. F., Vasconcelos, T. G., Henriques, D. M., Frank, C. D. S., König, A. & Kümmerer, K. 2008 Concentration of ciprofloxacin in Brazilian hospital effluent and preliminary risk assessment: a case study. *Clean Soil Air Water* **36** (3), 264–269.

Mitra, S., Das, S., Mandal, K. & Chaudhuri, S. 2007 Synthesis of a $\alpha$-$Fe_2O_3$ nanocrystal in its different morphological attributes: growth mechanism, optical and magnetic properties. *Nanotechnology* **18** (27), 1–9.

Muthumariappan, S. 2013 Synthesis and characterization of ciprofloxacin–zinc (II) complex and assay studies in pharmaceutical drugs. *J. Pharm. Res.* **6** (4), 437–441.

Nadeem, K., Traussnig, T., Letofsky-Papst, I., Krenn, H., Brossmann, U. & Würschum, R. 2010 Sol–gel synthesis and characterization of single-phase Ni ferrite nanoparticles dispersed in $SiO_2$ matrix. *J. Alloys Compd.* **493** (1), 385–390.

Nakamura, T. & Kubo, T. 1992 Tourmaline group crystals reaction with water. *Ferroelectrics* **137** (1), 13–31.

Pei, Z., Shan, X. Q., Kong, J., Wen, B. & Owens, G. 2009 Coadsorption of ciprofloxacin and Cu (II) on montmorillonite and kaolinite as affected by solution pH. *Environ. Sci. Technol.* **44** (3), 915–920.

Peng, X., Hu, F., Lam, F. L., Wang, Y., Liu, Z. & Dai, H. 2015 Adsorption behavior and mechanisms of ciprofloxacin from aqueous solution by ordered mesoporous carbon and bamboo-based carbon. *J. Colloid Interface Sci.* **460**, 349–360.

Picó, Y. & Andreu, V. 2007 Fluoroquinolones in soil – risks and challenges. *Anal. Bioanal. Chem.* **387** (4), 1287–1299.

Polishchuk, A. V., Karaseva, É. T., Emelina, T. B., Nikolenko, Y. M. & Karasev, V. E. 2009 Electronic structure and spectroscopic properties of norfloxacin, enrofloxacin, and nalidixic acid. *J. Struct. Chem.* **50** (3), 434–438.

Rakshit, S., Sarkar, D., Elzinga, E. J., Punamiya, P. & Datta, R. 2013 Mechanisms of ciprofloxacin removal by nano-sized magnetite. *J. Hazard. Mater.* **246**, 221–226.

Sadasivam, S., Krishna, S. K., Ponnusamy, K., Nagarajan, G. S., Kang, T. W. & Venkatesalu, S. C. 2010 Equilibrium and thermodynamic studies on the adsorption of an organophosphorous pesticide onto 'waste' jute fiber carbon. *J. Chem. Eng. Data* **55** (12), 5658–5662.

Sarmah, A. K., Meyer, M. T. & Boxall, A. B. A. 2006 A global perspective on the use, sales, exposure pathways, occurrence, fate and effects of veterinary antibiotics (VAs) in the environment. *Chemosphere* **65** (5), 725–759.

Sergei, V. S. & Alice, V. 2002 Electric induced transition in water cluster. *J. Mol. Struct.* **593**, 19–32.

Srivastava, V. C., Swamy, M. M., Mall, I. D., Prasad, B. & Mishra, I. M. 2006 Adsorptive removal of phenol by bagasse fly ash and activated carbon: equilibrium, kinetics and thermodynamics. *Colloids Surf. A Physicochem. Eng. Asp.* **272** (1), 89–104.

Sun, Y., Li, H., Li, G., Gao, B., Yue, Q. & Li, X. 2016 Characterization and ciprofloxacin adsorption properties of activated carbons prepared from biomass wastes by $H_3PO_4$ activation. *Bioresour. Technol.* **217**, 1–6.

Teske, S. S. & Arnold, R. G. 2008 Removal of natural and xeno-estrogens during conventional wastewater treatment. *Rev. Environ. Sci. Biotechnol.* **7** (2), 107–124.

Vasudevan, D., Bruland, G. L., Torrance, B. S., Upchurch, V. G. & MacKay, A. A. 2009 pH-dependent ciprofloxacin sorption to soils: interaction mechanisms and soil factors influencing sorption. *Geoderma* **51** (3), 68–76.

Wan, M., Li, Z., Hong, H. & Wu, Q. 2013 Enrofloxacin uptake and retention on different types of clays. *J. Asian Earth Sci.* **77**, 287–294.

Wang, C., Liu, J., Zhang, Z., Wang, B. & Sun, H. 2012 Adsorption of Cd (II), Ni (II), and Zn (II) by tourmaline at acidic conditions: kinetics, thermodynamics, and mechanisms. *Ind. Eng. Chem. Res.* **51** (11), 4397–4406.

Wang, C., Zhang, Y., Yu, L., Zhang, Z. & Sun, H. 2013 Oxidative degradation of azo dyes using tourmaline. *J. Hazard. Mater.* **260**, 851–859.

Wu, Y. F., Zhang, L., Mao, J. W., Liu, S. W., Huang, J., You, Y. R. & Mei, L. H. 2016 Kinetic and thermodynamic studies of sulforaphane adsorption on macroporous resin. *J. Chromatogr. B Analyt. Technol. Biomed. Life Sci.* **1028**, 231–236.

Xia, M. S., Hu, C. H. & Zhang, H. M. 2006 Effects of tourmaline addition on the dehydrogenase activity of Rhodopseudomonas palustris. *Process Biochem.* **41** (1), 221–225.

Xu, H. Y., Prasad, M. & Liu, Y. 2009 Schorl: a novel catalyst in mineral-catalyzed Fenton-like system for dyeing wastewater discoloration. *J. Hazard. Mater.* **165** (1), 1186–1192.

Yang, J. F., Ying, G. G., Zhao, J. L., Tao, R., Su, H. C. & Chen, F. 2010 Simultaneous determination of four classes of antibiotics in sediments of the Pearl Rivers using RRLC–MS/MS. *Sci. Total Environ.* **408** (16), 3424–3432.

Yu, L., Wang, C., Ren, X. & Sun, H. 2014 Catalytic oxidative degradation of bisphenol A using an ultrasonic-assisted tourmaline-based system: influence factors and mechanism study. *Chem. Eng. J.* **252**, 346–354.

Yu, F., Sun, S., Han, S., Zheng, J. & Ma, J. 2016 Adsorption removal of ciprofloxacin by multi-walled carbon nanotubes with different oxygen contents from aqueous solutions. *Chem. Eng. J.* **285**, 588–595.

Zhang, H. & Huang, C. H. 2007 Adsorption and oxidation of fluoroquinolone antibacterial agents and structurally related amines with goethite. *Chemosphere* **66**, 1502–1512.

Zhang, H., Li, G., Jia, Y. & Liu, H. 2009 Adsorptive removal of nitrogen-containing compounds from fuel. *J. Chem. Eng. Data* **55** (1), 173–177.

Zhang, C. L., Qiao, G. L., Zhao, F. & Wang, Y. 2011 Thermodynamic and kinetic parameters of ciprofloxacin adsorption onto modified coal Fly ash from aqueous solution. *J. Mol. Liq.* **163** (1), 53–56.

Zhang, Y., Cai, X., Lang, X., Qiao, X., Li, X. & Chen, J. 2012 Insights into aquatic toxicities of the antibiotics oxytetracycline and ciprofloxacin in the presence of metal: complexation versus mixture. *Environ. Pollut.* **166**, 48–56.

Zhang, Q. Q., Ying, G. G., Pan, C. G., Liu, Y. S. & Zhao, J. L. 2015 Comprehensive evaluation of antibiotics emission and fate in the river basins of China: source analysis, multimedia modeling, and linkage to bacterial resistance. *Environ. Sci. Technol.* **49** (11), 6772–6782.

First received 10 August 2016; accepted in revised form 23 January 2017. Available online 10 March 2017